RESEARCH PAPER

OncoImmunology 1:4, 419–431; July 2012; © 2012 Landes Bioscience

Combined vaccination and immunostimulatory antibodies provides durable cure of murine melanoma and induces transcriptional changes associated with positive outcome in human melanoma patients

A.J. Robert McGray, Dannie Bernard, Robin Hallett, Ryan Kelly, Mayank Jha, Caitlin Gregory, Jennifer D. Bassett, John A. Hassell, Guillaume Pare, Yonghong Wan and Jonathan L. Bramson*

Department of Pathology and Molecular Medicine; McMaster University; Hamilton, ON Canada

Keywords: T lymphocyte, vaccine, immune suppression, 4-1BB, PD-1, gene profiling

We have developed a recombinant adenovirus vaccine encoding dopachrome tautomerase (rHuAd5-hDCT) that produces robust DCT-specific immunity, but only provides modest suppression of murine melanoma. In the current study, an agonist antibody against 4-1BB was shown to enhance rHuAd5-hDCT efficacy and evoke tumor regression, but most tumors ultimately relapsed. The vaccine triggered upregulation of the immune inhibitory PD-1 signaling pathway and PD-1 blockade dramatically enhanced the rHuAd5-hDCT + anti-4-1BB strategy, resulting in complete regression of growing tumors in > 70% of recipients. The impact of the combined anti-4-1BB/anti-PD-1 treatment did not manifest as a dramatic enhancement in either the magnitude or functionality of DCT-specific tumor infiltrating lymphocytes relative to either treatment alone. Rather, a synergistic enhancement in intratumoral cytokine expression was observed, suggesting that the benefit of the combined therapy was a local event within the tumor. Global transcriptional analysis revealed immunological changes within the tumor following the curative vaccination, which extended beyond the T cell compartment. We identified an immune signature of 85 genes associated with clearance of murine melanoma that correlated with improved survival outcome in two independent cohorts of human melanoma patients. Our data reinforce the concept that successful vaccination must overcome local hurdles in the tumor microenvironment that are not manifest within the periphery. Further, tumor rejection following vaccination involves more than simply T cells. Finally, the association of our immune signature with positive survival outcome in human melanoma patients suggests that similar vaccination strategies may be promising for melanoma treatment.

Introduction

T cells play a key role in immune surveillance and tumor rejection. Although immune tolerance limits the availability of tumor-reactive T cells, anti-tumor T-cell responses can be generated using recombinant viral vaccines.[1,2] We have demonstrated that vaccination with a recombinant human adenovirus serotype 5 (rHuAd5) vector expressing the human dopachrome tautomerase antigen (hDCT; vector: rHuAd5-hDCT) elicited robust protection against the B16F10 murine melanoma in prophylactic and neo-adjuvant settings.[3-6] The same vaccine, however, only provided modest therapeutic benefit against growing tumors.[6,7] Although the mechanisms that limit the vaccine's activity against growing tumors remain to be determined, we have observed that the DCT-specific T-cell response evoked by immunizing naïve animals is of greater magnitude than the DCT response achieved in tumor-bearing mice, demonstrating that the tumor imposes a constraint on vaccine immunogenicity.[7]

T cells elaborate multiple effector functions that lead to tumor destruction, a property termed polyfunctionality, including the secretion of cytotoxic granules[8] and the production of IFNγ and TNFα.[9-12] In the presence of high antigen burden, such as the case of the tumor bed, T cells become impaired and lose their polyfunctionality.[13] We have observed this phenomenon in B16F10 tumors, where the polyfunctionality of DCT-specific tumor infiltrating lymphocytes (TIL) was markedly diminished in comparison to peripheral T cells.[7] Strategies to reverse this impairment would be expected to enhance the therapeutic effect of cancer vaccines.

Maximizing the activity of cancer vaccines necessitates an appreciation of the complex regulatory pathways that control the

*Correspondence to: Jonathan L. Bramson; Email: bramsonj@mcmaster.ca
Submitted: 01/25/12; Accepted: 01/30/12
http://dx.doi.org/10.4161/onci.19534

T-cell response. Following ligation of the antigen receptor, T-cell activation and function is regulated by costimulatory receptors of the TNFR and CD28 families.[14,15] Of particular interest to our study is the TNFR family member, 4-1BB, that plays a key role in T-cell proliferation,[16,17] effector function,[18] and memory formation.[19] Agonist 4-1BB monoclonal antibodies, used alone or with cancer vaccines, can improve T-cell immunity against poorly immunogenic tumors.[17,20-22] Of equal interest is PD-1, a CD28 family member that negatively regulates T cell function. PD-1 plays a role in limiting immune pathology[23] and is upregulated on T cells exposed to high antigen levels, such as tumor infiltrating lymphocytes.[24,25] Antagonists of PD-1 signaling can partially reverse T cell exhaustion and improve T-cell-mediated control of tumor growth.[26-28]

In this manuscript, we have employed immunomodulatory antibodies to enhance the efficacy of rHuAd5-hDCT. Treatment with a 4-1BB agonist following vaccination markedly increased the frequency of DCT-specific CD8$^+$ T cells, but only produced transient tumor regression. Blockade of PD-1 signaling also enhanced vaccine efficacy but complete tumor regression was only achieved when 4-1BB co-stimulation was combined with PD-1 blockade. Strikingly, the benefit of the combined immunomodulatory antibodies did not manifest as a dramatic alteration in T-cell polyfunctionality despite evidence of a synergistic enhancement of immune activity within the tumor. In fact, global transcriptional analysis of the tumor following curative vaccination revealed significant upregulation of a gene signature that extended beyond T cells, indicating that successful tumor rejection following vaccination requires more than simply vaccine-induced T cells.

Results

Increased 4-1BB signaling can improve immune attack resulting in enhanced rHuAd5-hDCT efficacy. We hypothesized that the limited anti-tumor efficacy of rHuAd5-hDCT could be improved by employing an agonist monoclonal antibody against 4-1BB (α4-1BB), based on reports that this agonist could enhance genetic vaccines[20,21,29,30] and recover TIL function.[31] 4-1BB expression on CD8$^+$ T cells was found to peak 5 d post-immunization with rHuAd5 and administration of the agonist mAb 5 d following rHuAd5 immunization could enhance the frequency of antigen-specific CD8$^+$ T cells in tumor-free mice (data not shown). Similar outcomes were observed with 100 μg–500 μg of α4-1BB (data not shown), therefore we employed a dose of 200 μg delivered on day 5 post-immunization for these experiments. Immunization of tumor-bearing mice with rHuAd5-hDCT + α4-1BB elicited a DCT-specific CD8$^+$ T cell response that was 8.7-fold greater than rHuAd5-hDCT alone in the peripheral blood (**Fig. 1A**) which was associated with transient tumor regression (**Fig. 1B**) and improved overall survival (**Fig. 1C**); however, most tumors ultimately relapsed. It is notable that progressive autoimmune vitiligo was observed in mice that experienced complete tumor regression (**Fig. 1D**). Treatment with α4-1BB in combination with an irrelevant vaccine, rHuAd5-LCMV-GP, did not elicit DCT-specific CD8$^+$ T cells (**Fig. 1A**) and had no impact on tumor growth or survival relative to untreated mice (**Fig. 1C** and data not shown). To gain further insight into the events within the tumor, we measured the expression of the T-cell-associated cytokines, IFNγ and TNFα, within the treated tumors. Whole tumor RNA was prepared from mice that were vaccinated with rHuAd5-hDCT +/– α4-1BB or the control vaccine rHuAd5-LCMV-GP + α4-1BB and cytokine expression was measured by qRT-PCR. Whereas cytokine expression in the tumors from mice immunized with rHuAd5-hDCT alone peaked 5–7 d post-vaccination and subsequently declined (**Fig. 1E**, broken line), treatment of tumor-bearing mice with the vaccine and α4-1BB significantly enhanced immune attack within the tumor (**Fig. 1E**). Interestingly, TNFα production was increased to a higher level than IFNγ. The elevation in cytokine expression was not due to the α4-1BB alone since tumors from mice treated with rHuAd5-LCMV-GP in combination with α4-1BB revealed no change in cytokine expression compared with untreated tumors (**Fig. 1F**). Expression of both IFNγ and TNFα persisted for a prolonged period when rHuAd5-hDCT was combined with α4-1BB, but began to decline around the same time point that the tumors relapsed.

Therapeutic vaccination with rHuAd5-hDCT promotes upregulation of the PD-1 signaling pathway within treated tumors. The immunosuppressive receptor PD-1 is often upregulated on CD8$^+$ T cells faced with a high antigen burden, as in the case of the tumor microenvironment,[24,25] so PD-1 expression was measured on vaccine-induced CD8$^+$ T cells in the peripheral blood (PBL) and within the tumor (TIL). While PD-1 expression was largely absent on DCT-specific CD8$^+$ PBL (**Fig. 2A**, upper left panels, gray histograms), PD-1 was significantly upregulated on DCT-specific CD8$^+$ TIL, irrespective of treatment with α4-1BB (**Fig. 2A**, upper right panels, gray histograms, rHuAd5-hDCT CD8$^+$ TIL MFI = 879.5 +/– 74.8, rHuAd5-hDCT + α4-1BB CD8$^+$ TIL MFI = 838.0 +/– 87.4). PD-1 expression by CD8$^+$ TIL required cognate interaction with tumor-associated antigen because LCMV-GP-specific CD8$^+$ PBL and TIL, which do not recognize antigen in B16F10 tumors, were both largely PD-1-negative, in the presence or absence of α4-1BB (**Fig. 2A**, lower panels, gray histograms, rHuAd5-LCMV-GP CD8$^+$ TIL MFI = 202.7 +/– 47.6, rHuAd5-LCMV-GP + α4-1**BB** CD8$^+$ TIL MFI = 238.8 +/– 41.7).

We also investigated expression of the PD-1 ligands, PD-L1 and PD-L2, in the tumor following immunization. Quantitative RT-PCR revealed that expression of PD-L1 and PD-L2 was significantly upregulated in the tumor following treatment with rHuAd5-hDCT +/– 4-1BB, but not in tumors from mice immunized with rHuAd5-LCMV GP +/– 4-1BB or left untreated (**Fig. 2B**), confirming the likelihood that PD-1 ligand/PD-1 interactions were limiting the anti-tumor function of tumor infiltrating CD8$^+$ T cells.

PD-1 blockade acts synergistically with 4-1BB co-stimulation to enhance immune attack within the tumor leading to complete tumor regression. Our data indicated that blockade of the PD-1 signaling pathway would be required to obtain the full benefit of the enhanced immunogenicity of the rHuAd5-hDCT + α4-1BB combination. Therefore, we combined the vaccination protocol

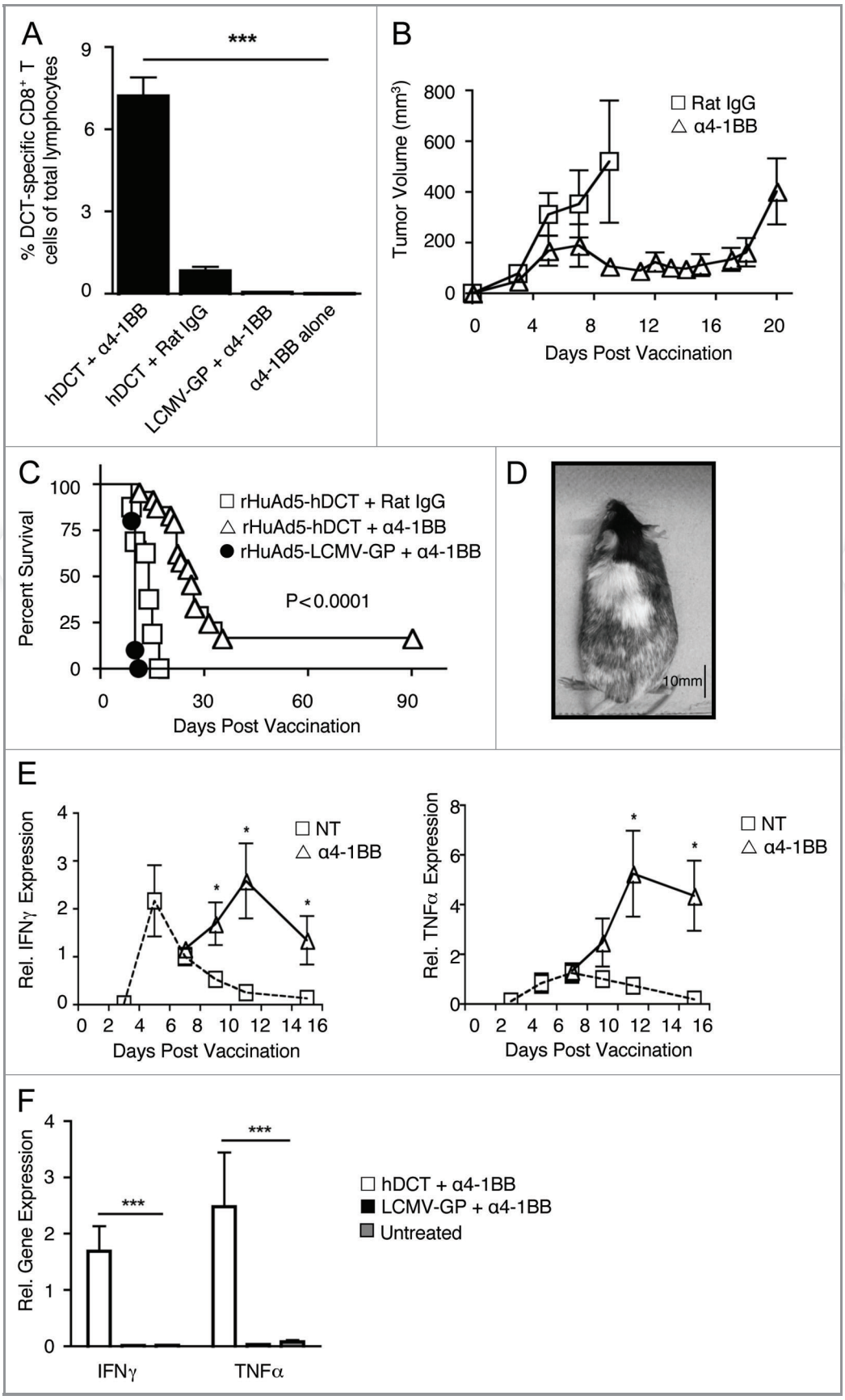

Figure 1. Stimulation of 4-1BB enhances the DCT-specific immune response following vaccination resulting in transient tumor regression and improved survival. (A) Tumor-bearing mice were immunized with rHuAd5-hDCT or rHuAd5-LCMV-GP and treated 5 d later with α4-1BB or Rat IgG. DCT-specific $CD8^+$ PBL were quantified 10 d post-vaccination (n = 5–20). (B and C) Tumor-bearing mice were immunized with rHuAd5-hDCT and treated with α4-1BB (△; n = 20) or Rat IgG (□; n = 9). As controls, mice were immunized with rHuAd5-LCMV-GP + α4-1BB (●; n = 8). (D) Example of progressive disseminated autoimmune vitiligo observed in cured mice following rHuAd5-hDCT + α4-1BB treatment. (E) Expression of IFNγ and TNFα in tumors from mice immunized with rHuAd5-hDCT + α4–1BB (△; n = 4–8) or rHuAd5-hDCT (□; n=4). (F) Expression of IFNγ and TNFα in tumors 9 d after treatment with rHuAd5-hDCT + α4-1BB (n = 7–9), rHuAd5-LCMV-GP + α4-1BB (n = 4) or untreated (n = 4). Tumor volumes were calculated from a single representative experiment (n = 4–5) and survival data was compiled from independent experiments. Data presented as mean +/− SEM.

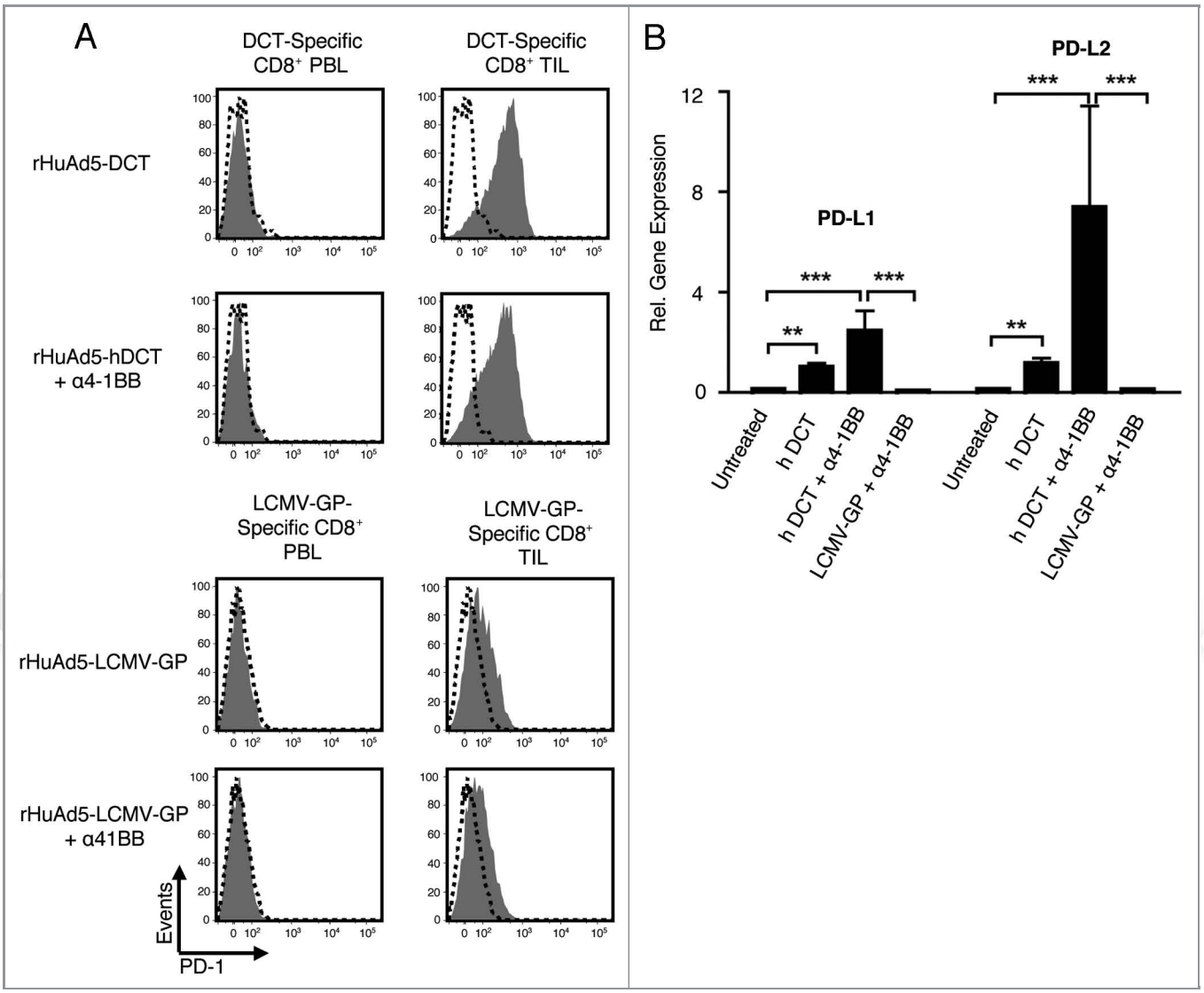

Figure 2. PD-1 is upregulated on tumor-specific CD8+ TIL following tumor infiltration in the context of elevated immunosuppressive PD-1 ligand expression in the tumor. (A) PD-1 was measured on antigen-specific CD8+ PBL and TIL (gray histograms) 10 d following immunization with rHuAd5-hDCT +/− α4-1BB or rHuAd5-LCMV-GP +/− α4-1BB. Dashed lines correspond to controls without PD-1 staining. Data presented from a single representative sample (n = 5–8). (B) Expression of PD-L1 and PD-L2 in tumors from mice left untreated (n = 4), treated rHuAd5-hDCT +/− α4-1BB (n = 4–8), or rHuAd5-LCMV-GP + α4-1BB (n = 4). Data presented as mean +/− SEM.

with an antagonist monoclonal antibody to block PD-1 signaling (αPD-1), delivered every third day beginning 3 d post vaccination. PD-1 blockade alone had no impact on the DCT-specific T-cell response produced by rHuAd5-hDCT (**Fig. 3A**), but the blockade did promote transient tumor regression (**Fig. 3B**), confirming the utility of the antibody to reverse local immune defects within the tumor. Strikingly, the combination of αPD-1 and α41-BB acted synergistically to enhance the efficacy of rHuAd5-hDCT, leading to complete regression of most tumors (**Fig. 3B**) despite no enhancement in the magnitude of the DCT-specific CD8+ T-cell response (**Fig. 3A**). This synergistic benefit manifested as a durable cure in > 70% of the mice, who remained tumor-free (**Fig. 3C**, $p < 0.0001$ compared with all other treatments); the cured mice subsequently developed progressive autoimmune vitiligo (**Fig. 3D**). Mice immunized with rHuAd5-LCMV-GP + α4-1BB + αPD-1 displayed no change in tumor growth (data not shown) or long-term survival (**Fig. 3C**, closed diamonds).

The therapeutic benefit of the combination therapy is not reflected in either the magnitude or functionality of the DCT-specific CD8+ TIL. To understand the benefit of the mAb combination, we investigated the DCT-specific CD8+ TIL following the various treatments. Strikingly, the combination treatments did not result in a significant change in the number of DCT-specific TIL compared with vaccination alone (**Fig. 4A**), suggesting that the observed differences in tumor growth were not due to increased infiltration of tumor-reactive T cells. The polyfunctionality of the DCT-specific CD8+ PBL and TIL was

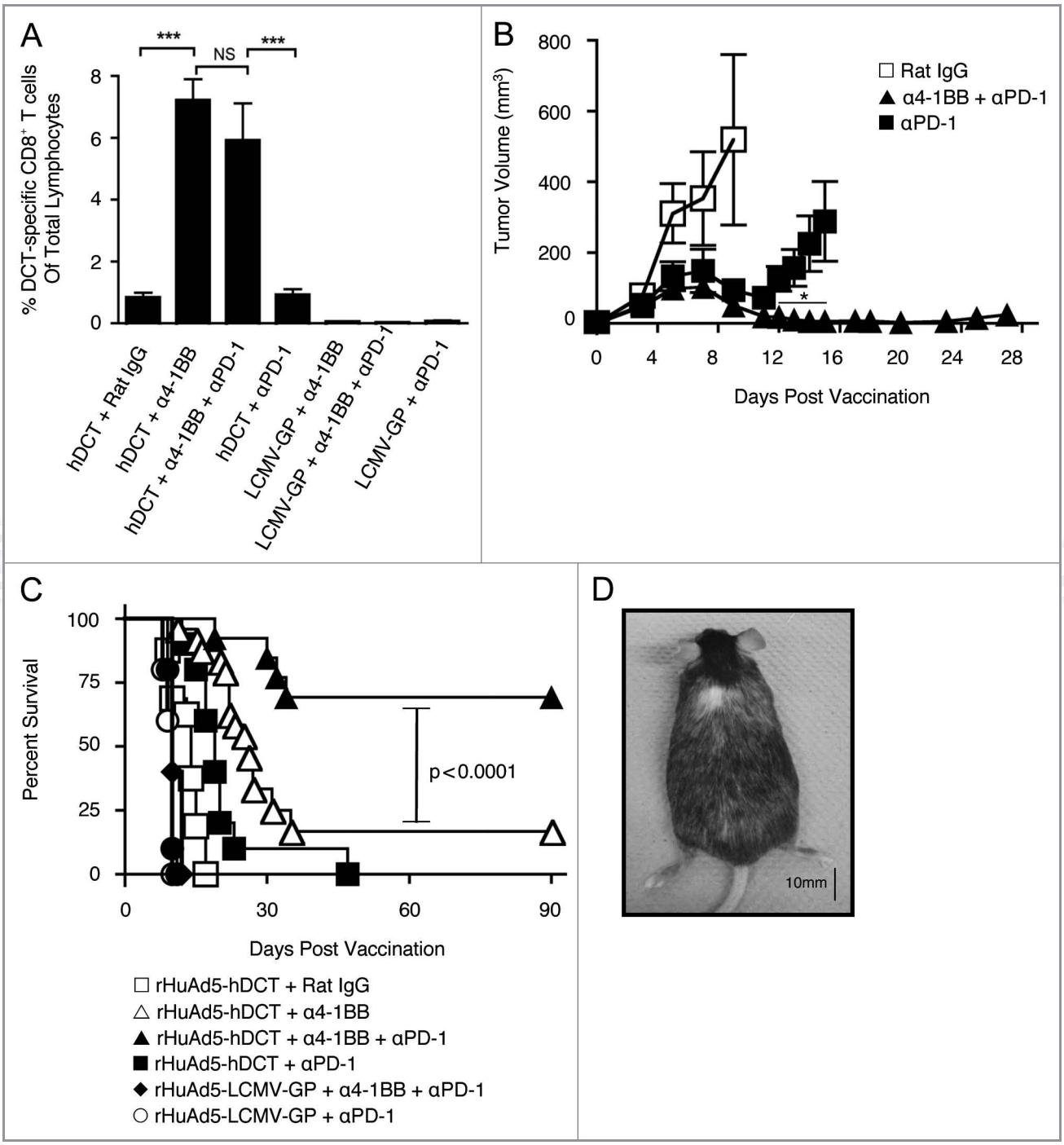

Figure 3. Vaccination combined with 4-1BB stimulation and PD-1 blockade results in complete tumor regression. (A) Tumor-bearing mice were immunized with rHuAd5-hDCT or rHuAd5-LCMV-GP and treated with α4-1BB and/or αPD-1 as indicated. DCT-specific CD8+ T cells were quantified in peripheral blood 10 d post vaccination (n = 3–20). rHuAd5-hDCT +/− α4-1BB data reproduced from **Figure 1** for reference. (B and C) Tumor-bearing mice were immunized with rHuAd5-hDCT + α4-1BB + αPD-1 (▲; n = 10), rHuAd5-hDCT + αPD-1 (■; n = 10) or rHuAd5-LCMV-GP + α4-1BB + αPD-1 (◆; n = 5) and rHuAd5-LCMV-GP + αPD-1 (○) (n = 5) as controls. rHuAd5-hDCT +/− α4-1BB survival data reproduced from **Figure 1** for reference. (D) Example of progressive disseminated autoimmune vitiligo observed in cured mice following rHuAd5-hDCT + α4-1BB + αPD-1 treatment. Tumor volumes were calculated from a single representative experiment (n = 4–5) and survival data was compiled from independent experiments. Data presented as mean +/− SEM.

examined to determine whether 4-1BB co-stimulation and/or PD-1 blockade reversed the previously described functional defects manifest in DCT-specific TIL.[7] Similar to our previous report,[7] the DCT-specific CD8+ T cells in the PBL were capable of producing multiple cytokines (IFNγ and TNFα) and undergoing degranulation (measured by mobilization of CD107a)

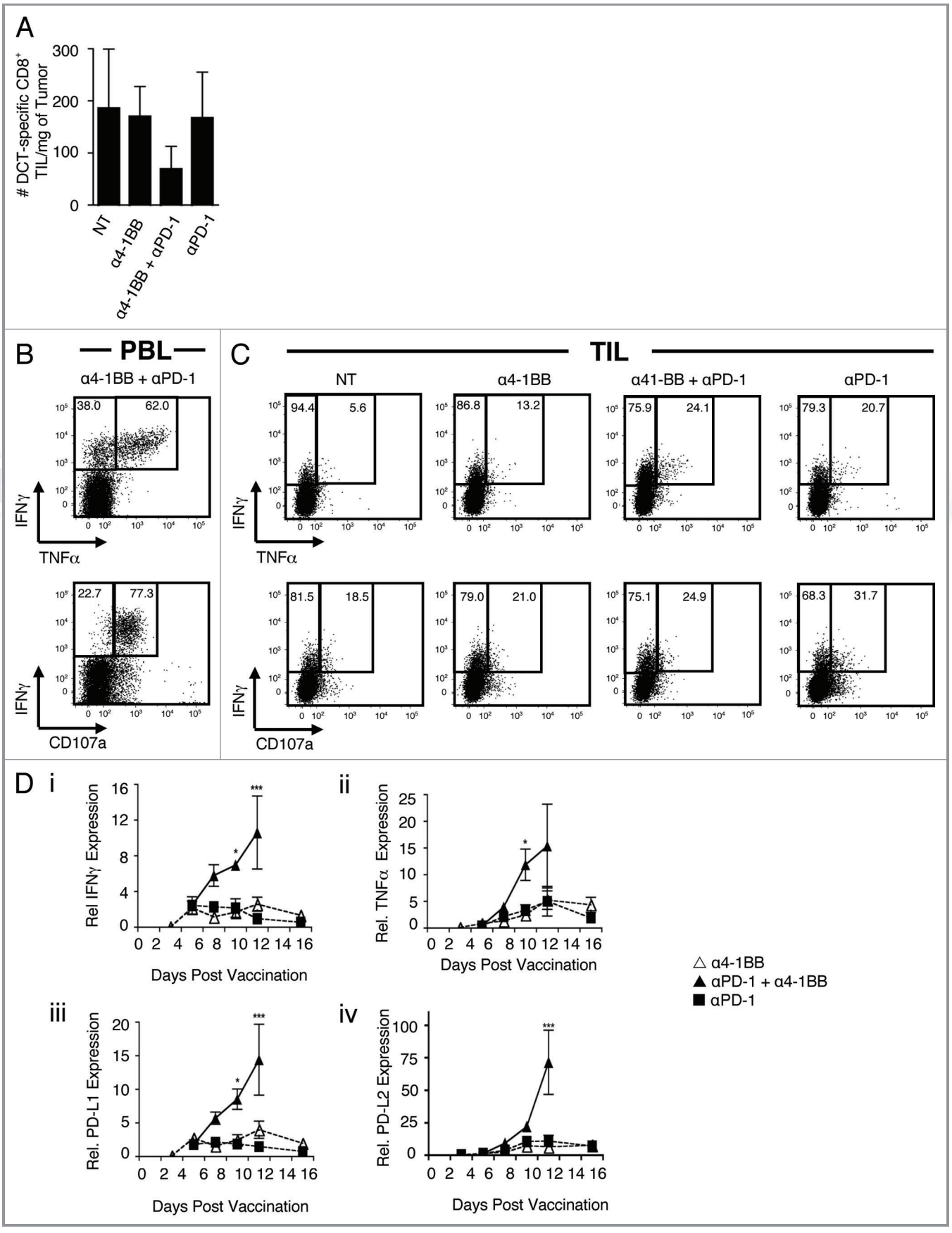
A
DCT-specific CD8+ TIL/mg of Tumor
300
200
100
0
NT
α4-1BB
α4-1BB + αPD-1
αPD-1
B
PBL
α4-1BB + αPD-1
38.0
62.0
IFNγ
TNFα
22.7
77.3
IFNγ
CD107a
C
TIL
NT
α4-1BB
α41-BB + αPD-1
αPD-1
94.4
5.6
86.8
13.2
75.9
24.1
79.3
20.7
IFNγ
TNFα
81.5
18.5
79.0
21.0
75.1
24.9
68.3
31.7
IFNγ
CD107a
D i
Rel IFNγ Expression
Days Post Vaccination
ii
Rel. TNFα Expression
Days Post Vaccination
iii
Rel. PD-L1 Expression
Days Post Vaccination
iv
Rel. PD-L2 Expression
Days Post Vaccination
α4-1BB
αPD-1 + α4-1BB
αPD-1

Figure 4 (See opposite page). 4-1BB co-stimulation and PD-1 blockade following vaccination synergize to increase immune activity within the tumor, despite no increase in the number of DCT-specific $CD8^+$ T cells and only limited improvements in T cell polyfunctionality. (A) Tumor-bearing mice were immunized with rHuAd5-hDCT and treated with α4-1BB, α4-1BB + αPD1, αPD-1 alone, or were given no additional treatment. DCT-specific $CD8^+$ TIL were quantified 10 d post-vaccination (n = 5 per treatment group). (B) Representative flow cytometric analysis of IFNγ and TNFα production and CD107a mobilization from DCT-specific $CD8^+$ PBL following rHuAd5hDCT + α4-1BB + αPD-1 treatment as described in (A). Values correspond to mean values calculated from compiled data (n = 9–19). (C) Representative flow cytometric analysis of IFNγ and TNFα production and CD107a mobilization by DCT-specific $CD8^+$ TIL for all treatments described in (A) (n = 5 per treatment group). Values correspond to mean values calculated from compiled data. Data presented as mean +/− SEM. (D) Expression of IFNγ, TNFα, PD-L1, and PD-L2 in tumors from mice treated with rHuAd5-hDCT in combination with α4-1BB (△), α4-1BB + αPD-1 (▲), or αPD-1 (■) (n = 4–8). α4-1BB data reproduced from **Figure 1** for reference.

(**Fig. 4B**), while the DCT-specific $CD8^+$ TIL were compromised in their ability to produce TNFα and degranulate (**Fig. 4C**). We noted small, but significant, increases in TIL functionality in groups receiving the PD-1 mAb, as measured by increased frequencies of $IFN\gamma^+/TNF\alpha^+$ and $IFN\gamma^+/CD107a^+$ $CD8^+$ TIL, suggesting that PD-1 blockade can recover some functionality in the vaccine-induced TIL. However, the change in polyfunctionality was not significantly different between mice who received αPD-1 alone and those that received α4-1BB + αPD-1, indicating that this modest enhancement in polyfunctionality could not explain the dramatic therapeutic effect.

Intratumoral transcriptional analysis reveals synergistic enhancement of local T cell activity upon inclusion of α4-1BB/αPD-1 treatment. We previously observed that intratumoral production of IFNγ and TNFα correlated with therapeutic outcome (**Fig. 1E**), therefore, to determine whether the combination therapy was associated with enhanced immune attack within the tumor, whole tumor RNA was isolated at discrete time intervals following treatment with rHuAd5-hDCT or rHuAd5-hDCT in combination with α4-1BB and/or αPD-1. Whereas treatment with rHuAd5-hDCT + α4-1BB or αPD-1 alone only resulted in transient elevation of IFNγ and TNFα expression within the tumor relative to treatment with rHuAd5-hDCT alone (**Fig. 4Di and ii** and data not shown), the combination of α4-1BB and αPD-1 produced a synergistic enhancement of cytokine expression relative to treatment with the individual mAbs (**Fig. 4Di and ii**). Further, the cytokine expression produced by the combination treatment continued to escalate until the tumors were too small to successfully retrieve RNA (day 14), while the cytokine expression in the mice receiving single mAbs plateaued and, ultimately, declined as the tumors relapsed. We also observed a synergistic enhancement in the expression of the PD-1 ligands PD-L1 and PD-L2, reinforcing the reciprocity between immune attack and upregulation of immune suppressive pathways in the tumor (**Fig. 4Diii and iv**).

Gene expression profiling of treated tumors reveals molecular differences between vaccine treatment groups. Our results thus far demonstrated that the combination therapy produces complete tumor regression and a profound immune attack within the tumor (as measured by IFNγ and TNFα production). Yet, this enhanced intratumoral immunity was not associated with a remarkable change in the DCT-specific $CD8^+$ TIL. To gain further insight into the mechanisms underlying the synergistic enhancements achieved through the combination treatment, we evaluated global transcriptional differences among tumors comprising each of the four treatment groups (rHuAd5-hDCT +/− α4-1BB and/or αPD-1). RNA was isolated from whole tumors 9 d post-vaccination and gene expression analyses were conducted using three biological replicates for each treatment group (n = 12). To gain insight into the biological differences between the treatment groups, we first identified the top 25 genes associated with each treatment using prediction analysis of microarrays (PAM), and completed a Gene Ontology (GO) analysis[32] (**Fig. 5A**; **Table S1**). GO analysis (**Table 1**) revealed that several immune related processes were enriched in rHuAd5-hDCT + α4-1BB + αPD-1 treated tumors, whereas cell survival programs such as the negative regulation of apoptosis or JNK signaling were enriched in the rHuAd5-hDCT treated tumors. Interestingly, this suggests that treatment with the rHuAd5-hDCT vaccine alone did not induce strong immunity against the tumor, but rather resulted in activation of tumor cell survival processes. Conversely, inclusion of + α4-1BB + αPD-1 with the vaccine was sufficient to induce tumor immunity and overcame the activation of survival processes.

Taken together, these transcriptional analyses suggest that the combination of rHuAd5-hDCT with + α4-1BB + αPD-1 not only results in induction of strong anti-tumor immunity, but also overcomes the activation of tumor cell survival processes associated with rHuAd5-hDCT treatment alone.

Treatment-induced changes in gene expression are associated with good clinical outcome in human melanoma patients. Our data suggest that rHuAd5-hDCT + α4-1BB + αPD-1 treatment elicited durable cures through complex immunological mechanisms which seem to involve both T cell-dependent and independent processes. We hypothesized that these same processes may be involved in the clinical course of human melanoma. To this end, we identified differentially expressed genes between rHuAd5-hDCT + α4-1BB +PD-1 treated tumors and all other treatment groups (**Fig. 6A**). We identified 94 differentially expressed Illumina probes, representing 85 unique genes, which we defined as the *immune-index* (**Fig. 6B and C**; **Table S2**).

To determine whether the biological changes embodied in our *immune-index* gene signature were consistent with observations in human melanoma patients, we interrogated the gene expression profiles of 123 metastatic melanoma samples (GSE19234, GSE22155) for which patient survival data was also available. Briefly, GSE19234 comprised 39 Stage III and 5 Stage IV metastatic melanomas, whereas GSE22155 comprised 79 Stage IV metastatic melanomas. Clinical outcome data was available for all 44 GSE19234 patients and 76 of 79 GSE22155 patients. Within the GSE19234 (**Fig. 6D**) cohort, patients with high immune-index scores experienced superior overall survival relative to those patients with lower immune index scores, and overall survival between these two groups was statistically different

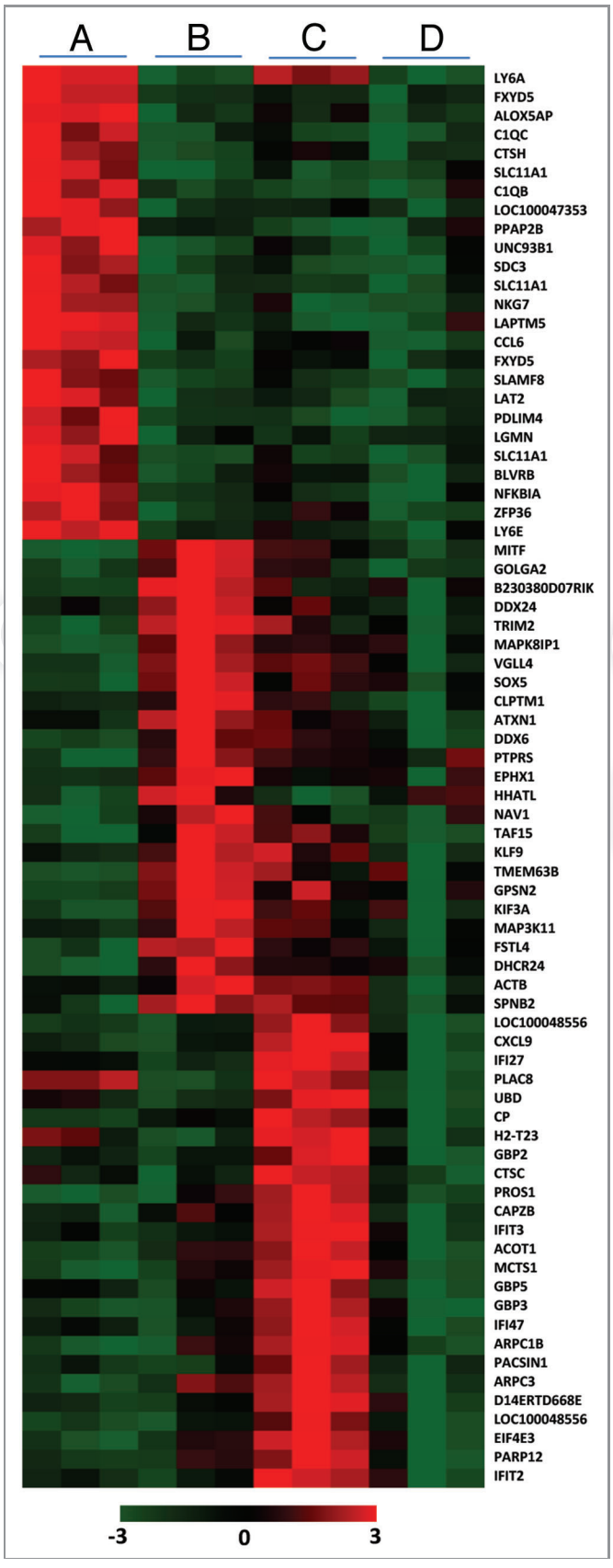

Figure 5. Identification of treatment specific probes. (A) PAM analysis was used to identify the top 25 probes associated with (A) rHuAd5-hDCT + α4-1BB + αPD-1, (B) rHuAd5-hDCT, and (C) rHuAd5-hDCT + α4-1BB. There were no probes which were specifically associated with the rHuAd5-hDCT + αPD-1 treatment (D).

(HR: 0.38, p = 0.018) (**Fig. 6E**) We observed a similar improvement in survival between immune-index high and immune-index low patients within the GSE22155 cohort (HR: 0.59, p = 0.035) (**Fig. 6F and G**). Overall, these observations demonstrate that the unique intratumoral biological processes induced by rHuAd5-hDCT + α4-1BB + αPD-1 treatment are associated with improved survival in two independent cohorts of human melanoma patients. Notably, these data suggest that cancer immunotherapies that elicit similar changes within human tumors may be beneficial in the treatment of melanoma patients.

Discussion

In the current study, we have addressed the limited efficacy of a prototypic cancer vaccine, rHuAd5-hDCT, against growing B16F10 melanomas. It has been suggested that the kinetics of the immune response elicited by vaccination may be too slow to

Table 1. Gene ontology biological process analysis of treatment specific genes

Gene Ontology – Biological Processes	
AdhDCT + 4-1BB + PD-1	**p**
Positive regulation of immune response	2.6 E-7
Positive regulation of response to stimulus	1.2 E-6
Activation of immune response	1.9 E-6
Positive regulation of immune system process	2.0 E-6
Leukocyte mediated immunity	1.2 E-4
AdhDCT	
Negative regulation of apoptosis	2.8 E-2
Negative regulation of programmed cell death	2.9 E-2
Negative regulation of cell death	2.9 E-2
Regulation of JNK cascade	4.9 E-2
Regulation of stress-activated protein kinase signaling pathway	5.0 E-2
AdhDCT + 4-1BB	
Immune response	3.8 E-4
Regulation of actin filament polymerization	1.8 E-3
Regulation of actin polymerization of depolymerization	2.2 E-3
Regulation of actin filament length	2.3 E-3
Regulation of protein polymerization	2.8 E-3
AdhDCT + PD-1 (Negative association genes, no positives)	
Immune response	1.6 E-4
Antigen processing and presentation of peptide antigen	7.6 E-4
Immunoglobulin mediated immune response	2.4 E-3
B-cell mediated immunity	2.6 E-3
Lymphocyte mediated immunity	3.5 E-3

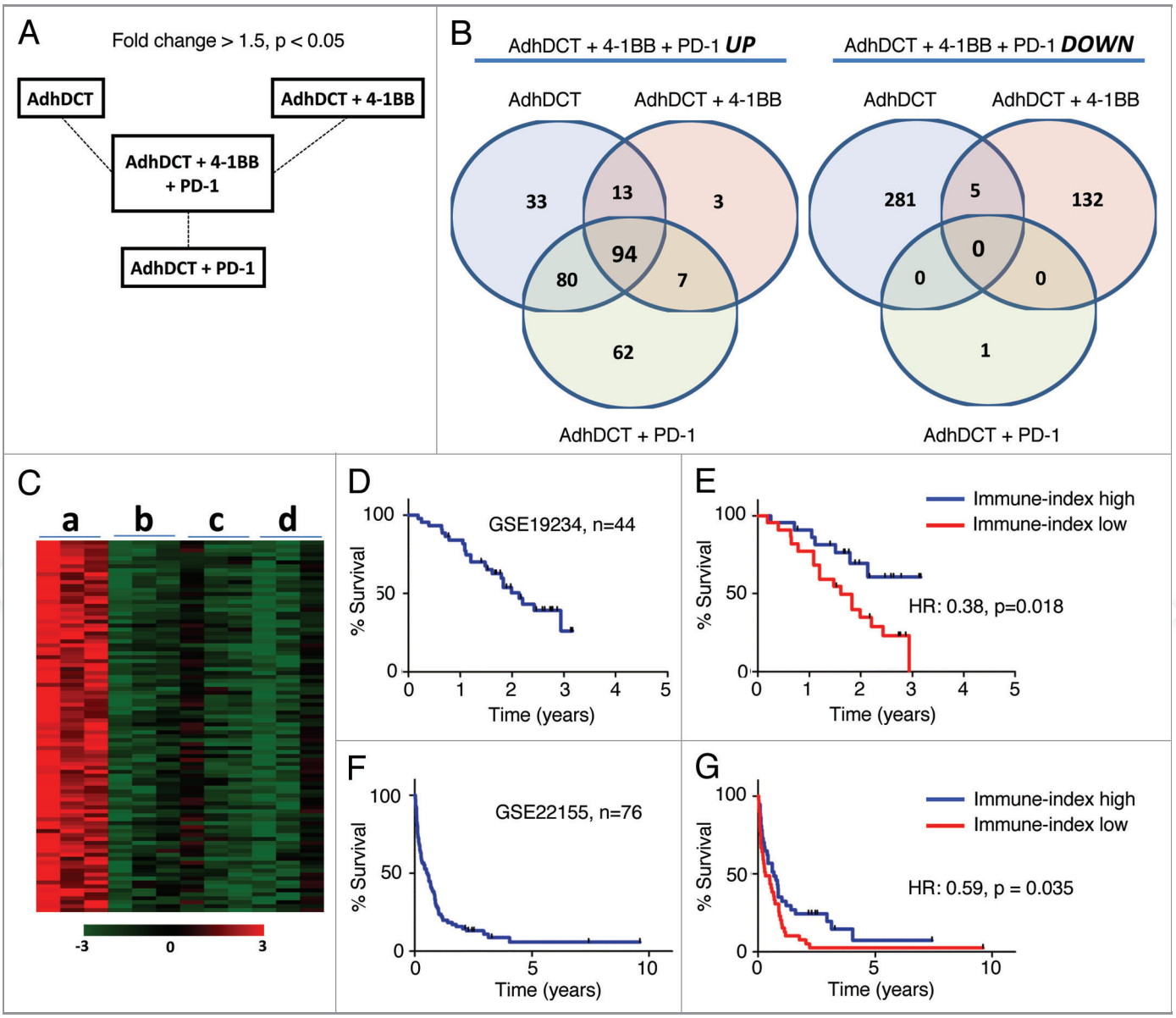

Figure 6. rHuAd5-hDCT + α4-1BB + αPD-1 treatment probes are associated with positive outcomes in human melanoma patients. (A) Summary of treatment comparisons to identify probes associated with treatment induced B16F10 tumor regression. (B) Probes that were differentially expressed in all comparisons are highlighted with Venn diagrams. Ninety-four probes were consistently overexpressed in the rHuAd5-hDCT + α4-1BB + αPD-1 treatment group relative to other treatments, whereas 0 probes were consistently under-expressed in the rHuAd5-hDCT + α4-1BB + αPD-1 treatment group relative to other treatments (Immune index). (C) Heatmap displaying expression levels of the 94 probes in each treatment group, (a) rHuAd5-hDCT + α4-1BB + αPD-1, (b) rHuAd5-hDCT, (c) rHuAd5-hDCT + α4-1BB, (d) rHuAd5-hDCT + αPD-1. (D–G) Kaplan-Meier survival curves for human patients with metastatic melanoma, (D) overall survival for 44 patients comprising the GSE19234 data set, (E) overall survival for the GSE19234 patient cohort divided into immune-index high and immune-index low groups (F) overall survival for 76 patients comprising the GSE22155 data set, (G) overall survival for the GSE22155 patient cohort divided into immune-index high and immune-index low groups.

significantly impact rapidly growing tumors like B16F10. However, our findings suggest that the true hurdle is the limited intratumoral immune activity elicited by the vaccine.

It is notable that under circumstances where we combined α4-1BB and αPD-1, we measured a synergistic increase in the production of IFNγ and TNFα within the tumor compared with treatment with either mAb on its own, despite no increase in tumor-specific TIL numbers or remarkable change in TIL polyfunctionality. This observation demonstrates that the true measure of vaccine activity requires analysis of intratumoral events and may not be apparent from ex vivo analysis of circulating T cells or TIL. This issue is of primary importance for extending vaccine strategies to humans as most studies rely upon sampling peripheral blood due to limited access to tumor tissues. Indeed, it is clear from this report and others[25,33] that T cells in the peripheral blood do not accurately reflect the cells in the tumor.

Our report goes further to demonstrate that ex vivo analysis of TIL may not provide an accurate measure of the events within the tumor either. Transcriptional analysis, however, provides an accurate and important measure of these events.

We have interpreted the expression of IFNγ and TNFα as evidence of T-cell activity; however, it is equally possible that other cell types, such as NK cells and macrophages, also contributed to the expression of these cytokines and, thus, the synergistic increase in local expression following treatment with combined α4-1BB and αPD-1 may be the result of activation of infiltrating populations other than T cells. Indeed monocytes, macrophages and NK cells can express both 4-1BB and PD-1 receptors,[34-36] supporting the possibility that the ultimate anti-tumor effect is due to the combined actions of these mAbs on T cells as well as non-T-cells. Further investigation is required to fully understand these mechanisms. As a step toward the elucidation of non-T-cell-dependent mechanisms, we examined global transcriptional changes in tumors that regressed and did not regress. Strikingly, the majority of the most highly over-expressed genes in the tumors from mice treated with the curative therapy were consistent with T-cell, macrophage/dendritic cell, and NK-cell infiltration, supporting a potential role for these cells in tumor clearance.

Using global transcriptional data, we defined a set of immune genes associated with tumors that undergo complete regression and applied this gene set to transcriptome data from metastatic melanoma samples taken from two natural history cohorts. Strikingly, our *immune-index* gene signature was found to be predictive of improved survival in human melanoma patients. It has previously been reported that tumors displaying an inflammatory phenotype are associated with improved prognosis in human melanoma patients through the use of similar transcriptional profiling approaches.[37-39] In the present study, we have identified a unique immune signature generated through the delivery of a pre-clinical immunotherapy in the context of a growing tumor that promotes tumor clearance. The observation that this immune signature is predictive of survival outcome in two independent cohorts of melanoma patients suggests that development of therapeutic interventions that produce similar changes of immune status in human melanoma tumor is worthy of further investigation. These data indicate that global transcriptional analysis is a useful tool to bridge the gap between preclinical discoveries and clinical challenges in humans. Further, this study supports the inclusion of transcriptional signatures derived from efficacious pre-clinical immunotherapy models as useful secondary clinical endpoints for cancer immunotherapy trials.

Overall, our findings further highlight the limitations of cancer vaccines and reinforce the concept that optimal delivery of cancer vaccines will require maximizing vaccine immunogenicity and suppressing negative regulators of T-cell function.[40] Our data also indicate that ex vivo analyses of PBL and TIL should be interpreted with caution since they do not accurately reflect the true immunological events within the tumor. Lastly, global analysis of vaccine treatment resulting in regression of murine tumors has revealed that similar immune signatures within human tumors are associated with good clinical outcome, further emphasizing the importance of understanding immunological changes within pre-clinical tumors as a means of improving the treatment of human cancer.

Materials and Methods

Mice. Female C57BL/6 mice were purchased from Charles River Breeding Laboratory. All of our investigations have been approved by the McMaster Animal Research Ethics Board.

Recombinant adenoviruses. The E1,E3-deleted recombinant human adenovirus serotype 5 (rHuAd5) vectors[41] used in this study have been described previously.[5,42] rHuAd5-hDCT expresses the full-length human dopachrome tautomerase (DCT) gene. rHuAd5-LCMV-GP encodes the dominant $CD8^+$ and $CD4^+$ T cell epitopes of the lymphocytic choriomeningitis virus glycoprotein.

Tumor challenge and immunization. Mice were challenged intradermally with 10^5 B16F10 cells. 10^8 pfu of Ad vector was prepared in 100 µl sterile PBS and injected in both rear thighs (50 µl/thigh) 5 d after tumor challenge. Tumor growth was monitored daily and measured with calipers every other day. Tumor volume was calculated as width × length × depth.

Isolation of tumor infiltrating lymphocytes. TIL were isolated as previously described.[7] Briefly, tumors were digested in a mixture of 0.5 mg/mL collagenase type I (Gibco), 0.2 mg/mL DNase (Roche) and 0.02 mg/mL hyalorunidase (Sigma) prepared in Hank's Buffered Saline (10 ml/250 mg of tumor). The digested material was passed successively through 70 µm and 40 µm nylon cell strainers and lymphocytes were purified using either mouse CD90.2 or CD45.2 positive selection by magnetic separation (EasySep, StemCell Technologies, Inc.).

Monoclonal antibodies. Anti-PD-1 (clone RMP1-14) was purchased from BioXcell and administered 3 d following vaccination using a schedule of 250 µg/mouse every 3 d[43] for a total of four injections. Anti-4-1BB was produced at McMaster University from the 3H3 hybridoma (kindly provided by Robert Mittler, Emory University) and administered to mice 5 d after vaccination at a dose of 200 µg/mouse. Total rat IgG (Sigma) was used as control. All flow cytometry antibodies (anti-CD16/CD32, anti-CD28, anti-CD4-PE-Cy7, anti-CD8α-PerCP-Cy5.5, anti-PD-1-PE, anti-CD107a-FITC, anti-IFNγ-APC and anti-TNFα-FITC) were purchased from BD Biosciences.

Intracellular cytokine staining (ICS). $CD8^+$ T-cell epitope peptides ($DCT_{180–188}$, $hDCT_{342–351}$, $hDCT_{363–371}$, LCMV-$GP_{31–43}$ and LCMV-$GP_{34–41}$) were purchased from Biomer Technologies, dissolved in DMSO and stored at -20°C. The ICS method has been described previously.[6] Briefly, lymphocytes were stimulated with either the DCT or LCMV-GP peptides (1 µg/mL) for 5 h at 37°C in the presence of 8 µg/mL anti-CD28 and 5 µg/mL brefeldin A (BD PharMingen). The CD107a mobilization assay was performed by adding anti-CD107a-FITC at the beginning of the peptide stimulation as described.[7] Data were acquired on a FACSCanto (BD Biosciences) and analyzed using FlowJo software (TreeStar).

RNA extraction from solid tumors and quantitative real-time PCR. Tumors were excised, snap-frozen in liquid nitrogen and stored at -80°C. Tumors were homogenized in Trizol (Invitrogen) using a Polytron PT 1200C (Kinematica) and total RNA was extracted according to the manufacturer's specifications. RNA samples were further purified using an RNeasy mini kit (Qiagen) and treated with Ambion's DNA-free kit. Reverse transcription was performed with Superscript III First-Strand (Invitrogen) according to the manufacturer's instructions. Quantitative PCR was performed on an ABI PRISM 7900HT Sequence Detection System (Applied Biosystems) using Perfecta SYBR Green SuperMix, ROX (Quanta Biosciences). Reaction efficiency was determined for individual primer sets using a minimum of five serial dilutions to ensure similar efficiency between target and endogenous control reactions. Data were analyzed via the delta/delta CT method using the Sequence Detector Software version 2.2 (Applied Biosystems). Primer sequences were as follows: IFNγ (FWD CTTGAAAGACAATCAGGCCATC; REV CAGCAGCGACTCCTTTTCC), TNFα (FWD AAATAG CTCCCAGAAAAGCAAG; REV CTGCCACAAGCAGGA ATGAG), PD-L1 (FWD AACCCGTGAGTGGGAAGAG; REV CCTGTTCTGTGGAGGATGTG) and PD-L2 (FWD ATAGGCAAGGAGCCCAGAAC; REV AACCCGGACTTC CCCTACAC). GAPDH (FWD AGGAGCGAGACCCCACTA AC; REV GGTTCACACCCATCACAAAC) was used as an endogenous control.

Illumina beadchip data. RNA from three independent B16F10 melanoma tumors was isolated (as described above) 9 d post-vaccination for each of the different treatment groups. (rHuAd-hDCT, rHuAd-hDCT + α4-1BB, rHuAd-hDCT + α4-1BB + αPD-1, rHuAd-hDCT + αPD-1) and prepared for profiling on MouseRef-8_V2 beadchips, according to manufacturer's protocol (Illumina). Treatment specific genes were determined using PAM analysis and the top 25 genes for each treatment group were used to complete a gene ontology analysis.[32]

Comparison with clinical melanoma samples. We calculated all Illumina probes which were consistently differentially expressed between the rHuAd-hDCT + α4-1BB + αPD-1 treated tumors and all other treatment groups (rHuAd-hDCT, rHuAd-hDCT + α4-1BB, rHuAd-hDCT + αPD-1). Genes were considered differentially expressed if the fold-change was > 1.5 and the p-value < 0.05 in each comparison (Two-tailed, unpaired Student's t-test).[44] Gene expression profiles of 123 melanoma tumors for which clinical outcome data was available were downloaded from the Gene Expression Omnibus [GEO, GSE22153 (n = 57, Illumina human-6 v2.0 expression beadchips),[38] GSE22154 (n = 22, Illumina HumanHT-12 V3.0 expression beadchips),[38] and GSE19234 (n = 44, Affymetrix HG-U133 Plus 2.0 arrays)].[37] All data sets were filtered such that when multiple probes recognized the same gene transcripts, only the probe with the highest mean intensity was used. For cross-platform comparisons, genes were mapped by Unigene IDs to either Affymetrix HG-U133 Plus 2.0 arrays, Illumina human-6 v2.0 expression beadchips, or Illumina HumanHT-12 V3.0 expression beadchips. Affymetrix array expression files were created from raw .cel files that were normalized using Robust Multi-Array Analysis (RMA).[45] Illumina expression files were created using the IlluminaExpressionFileCreator module available on Gene Pattern (http://genepattern.broadinstitute.org/gp/pages/index.jsf), similar to Illumina BeadStudio, from raw .IDAT files. The expression values for each gene were transformed such that the mean was 0 and the standard deviation was 1 within each individual data set. An immune index was calculated for each patient as follows:

$$\frac{\sum_{i \in P} x_i}{n_P} - \frac{\sum_{i \in N} x_j}{n_N} \quad (1)$$

Where x is the transformed expression, n is the number of genes that could be mapped between platforms, P is the set of probes with higher expression in rHuAd-hDCT + α4-1BB + αPD-1 treated tumors, and N is the set of probes with lower expression in rHuAd-hDCT + α4-1BB + αPD-1 treated tumors.[46] The median immune index value was used as the cut-point between high and low immune index values. Kaplan-Meier analysis was used to compare survival characteristics between patients with high and low immune indices.

Statistical analysis. Two-tailed, unpaired Student's t-tests were used to compare two treatment groups. One and two way Analysis of Variances (ANOVA) were used for data analysis of more than two groups and a Bonferroni post test was utilized to determine significant differences between treatment groups. Survival data was compared using a logrank test. Results were generated using GraphPad Prism 4.0b software. Differences between means were considered significant at $p < 0.05$: $^{*}p < 0.05$, $^{**}p < 0.01$, $^{***}p < 0.001$. NS: not significant.

Disclosure of Potential Conflicts of Interest

No potential conflicts of interest were disclosed.

Acknowledgments

This work was supported by funds from the Terry Fox Foundation. D.B. was supported by a scholarship from the Canadian Institutes for Health Research.

Supplemental Material

Supplemental materials may be found here:
www.landesbioscience.com/journals/oncoimmunology/article/19534/

References

1. Harrop R, John J, Carroll MW. Recombinant viral vectors: cancer vaccines. Adv Drug Deliv Rev 2006; 58:931-47; PMID:17030074; http://dx.doi.org/10.1016/j.addr.2006.05.005
2. Anderson RJ, Schneider J. Plasmid DNA and viral vector-based vaccines for the treatment of cancer. Vaccine 2007; 25(Suppl 2):B24-34; PMID:17698262; http://dx.doi.org/10.1016/j.vaccine.2007.05.030
3. Lane C, Leitch J, Tan X, Hadjati J, Bramson JL, Wan Y. Vaccination-induced autoimmune vitiligo is a consequence of secondary trauma to the skin. Cancer Res 2004; 64:1509-14; PMID:14973051; http://dx.doi.org/10.1158/0008-5472.CAN-03-3227
4. Kianizad K, Marshall LA, Grinshtein N, Bernard D, Margl R, Cheng S, et al. Elevated frequencies of self-reactive CD8$^+$ T cells following immunization with a xenoantigen are due to the presence of a heteroclitic CD4$^+$ T-cell helper epitope. Cancer Res 2007; 67: 6459-67; PMID:17616707; http://dx.doi.org/10.1158/0008-5472.CAN-06-4336
5. Bernard D, Ventresca MS, Marshall LA, Evelegh C, Wan Y, Bramson JL. Processing of tumor antigen differentially impacts the development of helper and effector CD4$^+$ T-cell responses. Mol Ther 2010; 18:1224-32; PMID:20179673; http://dx.doi.org/10.1038/mt.2010.30
6. Grinshtein N, Bridle B, Wan Y, Bramson JL. Neoadjuvant vaccination provides superior protection against tumor relapse following surgery compared with adjuvant vaccination. Cancer Res 2009; 69:3979-85; PMID:19383917; http://dx.doi.org/10.1158/0008-5472.CAN-08-3385
7. Grinshtein N, Ventresca M, Margl R, Bernard D, Yang TC, Millar JB, et al. High-dose chemotherapy augments the efficacy of recombinant adenovirus vaccines and improves the therapeutic outcome. Cancer Gene Ther 2009; 16:338-50; PMID:18989352; http://dx.doi.org/10.1038/cgt.2008.89
8. Lowin B, Hahne M, Mattmann C, Tschopp J. Cytolytic T-cell cytotoxicity is mediated through perforin and Fas lytic pathways. Nature 1994; 370: 650-2; PMID:7520535; http://dx.doi.org/10.1038/370650a0
9. Ashkenazi A, Dixit VM. Death receptors: signaling and modulation. Science 1998; 281:1305-8; PMID: 9721089; http://dx.doi.org/10.1126/science.281.5381.1305
10. Chawla-Sarkar M, Lindner DJ, Liu YF, Williams BR, Sen GC, Silverman RH, et al. Apoptosis and interferons: role of interferon-stimulated genes as mediators of apoptosis. Apoptosis 2003; 8:237-49; PMID:12766484; http://dx.doi.org/10.1023/A:1023668705040
11. Dalton DK, Pitts-Meek S, Keshav S, Figari IS, Bradley A, Stewart TA. Multiple defects of immune cell function in mice with disrupted interferon-gamma genes. Science 1993; 259:1739-42; PMID:8456300; http://dx.doi.org/10.1126/science.8456300
12. Wigginton JM, Gruys E, Geiselhart L, Subleski J, Komschlies KL, Park JW, et al. IFN-gamma and Fas/FasL are required for the antitumor and antiangiogenic effects of IL-12/pulse IL-2 therapy. J Clin Invest 2001; 108:51-62; PMID:11435457
13. Kim PS, Ahmed R. Features of responding T cells in cancer and chronic infection. Curr Opin Immunol 2010; 22:223-30; PMID:20207527; http://dx.doi.org/10.1016/j.coi.2010.02.005
14. Watts TH. TNF/TNFR family members in costimulation of T cell responses. Annu Rev Immunol 2005; 23:23-68; PMID:15771565; http://dx.doi.org/10.1146/annurev.immunol.23.021704.115839
15. Sharpe AH, Freeman GJ. The B7-CD28 superfamily. Nat Rev Immunol 2002; 2:116-26; PMID:11910893; http://dx.doi.org/10.1038/nri727
16. Shuford WW, Klussman K, Tritchler DD, Loo DT, Chalupny J, Siadak AW, et al. 4-1BB costimulatory signals preferentially induce CD8$^+$ T cell proliferation and lead to the amplification in vivo of cytotoxic T cell responses. J Exp Med 1997; 186:47-55; PMID: 9206996; http://dx.doi.org/10.1084/jem.186.1.47
17. Wilcox RA, Flies DB, Zhu G, Johnson AJ, Tamada K, Chapoval AI, et al. Provision of antigen and CD137 signaling breaks immunological ignorance, promoting regression of poorly immunogenic tumors. J Clin Invest 2002; 109:651-9; PMID:11877473
18. Kwon BS, Hurtado JC, Lee ZH, Kwack KB, Seo SK, Choi BK, et al. Immune responses in 4-1BB (CD137)-deficient mice. J Immunol 2002; 168:5483-90; PMID: 12023342
19. Takahashi C, Mittler RS, Vella AT. Cutting edge: 4-1BB is a bona fide CD8 T cell survival signal. J Immunol 1999; 162:5037-40; PMID:10227968
20. Melero I, Shuford WW, Newby SA, Aruffo A, Ledbetter JA, Hellström KE, et al. Monoclonal antibodies against the 4-1BB T-cell activation molecule eradicate established tumors. Nat Med 1997; 3:682-5; PMID:9176498; http://dx.doi.org/10.1038/nm0697-682
21. Ju SA, Lee SC, Kwon TH, Heo SK, Park SM, Paek HN, et al. Immunity to melanoma mediated by 4-1BB is associated with enhanced activity of tumour-infiltrating lymphocytes. Immunol Cell Biol 2005; 83:344-51; PMID:16033529; http://dx.doi.org/10.1111/j.1440-1711.2005.01330.x
22. Gray JC, French RR, James S, Al-Shamkhani A, Johnson PW, Glennie MJ. Optimising anti-tumour CD8 T-cell responses using combinations of immunomodulatory antibodies. Eur J Immunol 2008; 38:2499-511; PMID:18792403; http://dx.doi.org/10.1002/eji.200838208
23. Francisco LM, Sage PT, Sharpe AH. The PD-1 pathway in tolerance and autoimmunity. Immunol Rev 2010; 236:219-42; PMID:20636820; http://dx.doi.org/10.1111/j.1600-065X.2010.00923.x
24. Thompson RH, Dong H, Lohse CM, Leibovich BC, Blute ML, Cheville JC, et al. PD-1 is expressed by tumor-infiltrating immune cells and is associated with poor outcome for patients with renal cell carcinoma. Clin Cancer Res 2007; 13:1757-61; PMID:17363529; http://dx.doi.org/10.1158/1078-0432.CCR-06-2599
25. Ahmadzadeh M, Johnson LA, Heemskerk B, Wunderlich JR, Dudley ME, White DE, et al. Tumor antigen-specific CD8 T cells infiltrating the tumor express high levels of PD-1 and are functionally impaired. Blood 2009; 114:1537-44; PMID:19423728; http://dx.doi.org/10.1182/blood-2008-12-195792
26. Barber DL, Wherry EJ, Masopust D, Zhu B, Allison JP, Sharpe AH, et al. Restoring function in exhausted CD8 T cells during chronic viral infection. Nature 2006; 439:682-7; PMID:16382236; http://dx.doi.org/10.1038/nature04444
27. Li B, VanRoey M, Wang C, Chen TH, Korman A, Jooss K. Anti-programmed death-1 synergizes with granulocyte macrophage colony-stimulating factor–secreting tumor cell immunotherapy providing therapeutic benefit to mice with established tumors. Clin Cancer Res 2009; 15:1623-34; PMID:19208793; http://dx.doi.org/10.1158/1078-0432.CCR-08-1825
28. Pilon-Thomas S, Mackay A, Vohra N, Mulé JJ. Blockade of programmed death ligand 1 enhances the therapeutic efficacy of combination immunotherapy against melanoma. J Immunol 2010; 184:3442-9; PMID:20194714; http://dx.doi.org/10.4049/jimmunol.0904114
29. Miller RE, Jones J, Le T, Whitmore J, Boiani N, Gliniak B, et al. 4-1BB-specific monoclonal antibody promotes the generation of tumor-specific immune responses by direct activation of CD8 T cells in a CD40-dependent manner. J Immunol 2002; 169: 1792-800; PMID:12165501
30. Li B, Lin J, Vanroey M, Jure-Kunkel M, Jooss K. Established B16 tumors are rejected following treatment with GM-CSF-secreting tumor cell immunotherapy in combination with anti-4-1BB mAb. Clin Immunol 2007; 125:76-87; PMID:17706463; http://dx.doi.org/10.1016/j.clim.2007.07.005
31. Choi BK, Kim YH, Kang WJ, Lee SK, Kim KH, Shin SM, et al. Mechanisms involved in synergistic anti-cancer immunity of anti-4-1BB and anti-CD4 therapy. Cancer Res 2007; 67:8891-9; PMID:17875731; http://dx.doi.org/10.1158/0008-5472.CAN-07-1056
32. Tibshirani R, Hastie T, Narasimhan B, Chu G. Diagnosis of multiple cancer types by shrunken centroids of gene expression. Proc Natl Acad Sci U S A 2002; 99:6567-72; PMID:12011421; http://dx.doi.org/10.1073/pnas.082099299
33. Appay V, Jandus C, Voelter V, Reynard S, Coupland SE, Rimoldi D, et al. New generation vaccine induces effective melanoma-specific CD8$^+$ T cells in the circulation but not in the tumor site. J Immunol 2006; 177:1670-8; PMID:16849476
34. Vinay DS, Kwon BS. 4-1BB signaling beyond T cells. Cell Mol Immunol 2011; 8:281-4; PMID:21217771; http://dx.doi.org/10.1038/cmi.2010.82
35. Zhang Y, Ma CJ, Ni L, Zhang CL, Wu XY, Kumaraguru U, et al. Cross-talk between programmed death-1 and suppressor of cytokine signaling-1 in inhibition of IL-12 production by monocytes/macrophages in hepatitis C virus infection. J Immunol 2011; 186:3093-103; PMID:21263070; http://dx.doi.org/10.4049/jimmunol.1002006
36. Chen Y, Wu S, Guo G, Fei L, Guo S, Yang C, et al. Programmed death (PD)-1-deficient mice are extremely sensitive to murine hepatitis virus strain-3 (MHV-3) infection. PLoS Pathog 2011; 7:e1001347; PMID: 21750671; http://dx.doi.org/10.1371/journal.ppat.1001347
37. Bogunovic D, O'Neill DW, Belitskaya-Levy I, Vacic V, Yu YL, Adams S, et al. Immune profile and mitotic index of metastatic melanoma lesions enhance clinical staging in predicting patient survival. Proc Natl Acad Sci U S A 2009; 106:20429-34; PMID:19915147; http://dx.doi.org/10.1073/pnas.0905139106
38. Jönsson G, Busch C, Knappskog S, Geisler J, Miletic H, Ringnér M, et al. Gene expression profiling-based identification of molecular subtypes in stage IV melanomas with different clinical outcome. Clin Cancer Res 2010; 16:3356-67; PMID:20460471; http://dx.doi.org/10.1158/1078-0432.CCR-09-2509
39. Gajewski TF, Fuertes M, Spaapen R, Zheng Y, Kline J. Molecular profiling to identify relevant immune resistance mechanisms in the tumor microenvironment. Curr Opin Immunol 2011; 23:286-92; PMID: 21185705; http://dx.doi.org/10.1016/j.coi.2010.11.013
40. Lasaro MO, Ertl HC. Targeting inhibitory pathways in cancer immunotherapy. Curr Opin Immunol 2010; 22:385-90; PMID:20466529; http://dx.doi.org/10.1016/j.coi.2010.04.005
41. Ng P, Parks RJ, Cummings DT, Evelegh CM, Graham FL. An enhanced system for construction of adenoviral vectors by the two-plasmid rescue method. Hum Gene Ther 2000; 11:693-9; PMID:10757349; http://dx.doi.org/10.1089/10430340050015590
42. Leitch J, Fraser K, Lane C, Putzu K, Adema GJ, Zhang QJ, et al. CTL-dependent and -independent antitumor immunity is determined by the tumor not the vaccine. J Immunol 2004; 172:5200-5; PMID:15100257
43. Curran MA, Montalvo W, Yagita H, Allison JP. PD-1 and CTLA-4 combination blockade expands infiltrating T cells and reduces regulatory T and myeloid cells within B16 melanoma tumors. Proc Natl Acad Sci U S A 2010; 107:4275-80; PMID:20160101; http://dx.doi.org/10.1073/pnas.0915174107

44. Shi L, Jones WD, Jensen RV, Harris SC, Perkins RG, Goodsaid FM, et al. The balance of reproducibility, sensitivity, and specificity of lists of differentially expressed genes in microarray studies. BMC Bioinformatics 2008; 9(Suppl 9):S10; PMID:18793455; http://dx.doi.org/10.1186/1471-2105-9-S9-S10

45. Irizarry RA, Hobbs B, Collin F, Beazer-Barclay YD, Antonellis KJ, Scherf U, et al. Exploration, normalization, and summaries of high density oligonucleotide array probe level data. Biostatistics 2003; 4:249-64; PMID:12925520; http://dx.doi.org/10.1093/biostatistics/4.2.249

46. Yau C, Esserman L, Moore DH, Waldman F, Sninsky J, Benz CC. A multigene predictor of metastatic outcome in early stage hormone receptor-negative and triple-negative breast cancer. Breast Cancer Res 2010; 12:R85; PMID:20946665; http://dx.doi.org/10.1186/bcr2753